CHEMISTRY OF MATERIALS
Article

Chem. Mater. **2010,** *22,* 4531–4538 4531
DOI:10.1021/cm101778g

Controlled Multiscale Synthesis of Porous Coordination Polymer in Nano/Micro Regimes

Stéphane Diring,[†,‡] Shuhei Furukawa,*[,†,‡] Yohei Takashima,[§] Takaaki Tsuruoka,[†,∥] and Susumu Kitagawa*[,†,‡,§]

[†]*ERATO Kitagawa Integrated Pores Project, Japan Science and Technology Agency (JST), Kyoto Research Park Bldg #3, Shimogyo-ku, Kyoto 600-8815, Japan,* [‡]*Institute for Integrated Cell-Material Sciences (iCeMS), Kyoto University, Yoshida, Sakyo-ku, Kyoto 606-8501, Japan,* [§]*Department of Synthetic Chemistry and Biological Chemistry, Graduate School of Engineering, Kyoto University, Katsura, Nishikyo-ku, Kyoto 615-8510, Japan, and* [∥]*Frontiers of Innovative Research in Science and Technology (FIRST), Konan University, 7-1-20, Minatojima-minamimachi, Chuo-ku, Kobe 650-0047, Japan*

Received June 25, 2010

A simple and straightforward method combines microwave-assisted solvothermal conditions with the coordination modulation method to achieve the size-controlled formation of the porous coordination polymer (PCP), $[Cu_3(btc)_2]$ (where btc represents benzene-1,3,5-tricarboxylate) in the nano/micro regimes. The addition of a monocarboxylic acid modulator to the reaction mixture greatly influenced the morphology of the resulting sample, through competitive coordination interactions during the crystal formation process. By adjusting the concentration of dodecanoic acid additive, we could subtly control the nucleation rate of a $[Cu_3(btc)_2]$ framework and, thus, the resulting crystal size. Homogeneous nanocrystals of the PCP with sizes ranging from few tenths of nanometers up to few micrometers could be successfully obtained in a controlled manner. X-ray diffractions and gas sorption measurements revealed highly crystalline particles with large pore volumes. Moreover, variations in the sorption profiles could be correlated to the size and morphology of the $[Cu_3(btc)_2]$ samples, presenting affinity for gas condensation at high relative pressures or even hierarchical dual porous structures with mesoporous grain boundaries.

Introduction

Porous coordination polymers (PCPs) or metal−organic frameworks (MOFs) are a unique class of hybrid porous materials obtained from the assembly process between inorganic molecular building blocks and suitable organic linkers.[1−7] Over the last years, they have generated tremendous interest because of their potential in many applications such as gas storage,[8] separation,[9] and catalysis,[10] because their framework topologies and pore sizes can be designed for selective guest accommodation, and the functionality of the pore surfaces directly influences the interaction with guest molecules. To date, however, the research efforts have been mainly focused on bulk powder crystalline materials. This is because the intriguing porous properties are usually attributed to the PCPs framework structures themselves; therefore, all the investigation of properties is averaged over samples and the contribution of the crystal size and morphology has been rarely taken into account.

When the PCP crystals are downsized to nanometer scale, the contribution of the crystal interface is no longer negligible; simply in the cubic crystal morphology, the ratio of surface area over volume (S/V) can be denoted as $S/V = 6/a$, where a is the length of the side of cube. In the case of porous materials, the crystal interface can be expected to influence the sorption kinetics or even the

*Authors to whom correspondence should be addressed. E-mails: shuhei.furukawa@kip.jst.go.jp (S.F.), kitagawa@sbchem.kyoto-u.ac.jp (S.K.).

(1) Yaghi, O. M.; O'Keeffe, M.; Ockwig, N. W.; Chae, H. K.; Eddaoudi, M.; Kim, J. *Nature* **2003**, *423*, 705–714.
(2) Kitagawa, S.; Kitaura, R.; Noro, S. *Angew. Chem., Int. Ed.* **2004**, *43*, 2334–2375.
(3) Ferey, G.; Mellot-Draznieks, C.; Serre, C.; Millange, F. *Acc. Chem. Res.* **2005**, *38*, 217–225.
(4) Bradshaw, D.; Claridge, J. B.; Cussen, E. J.; Prior, T. J.; Rosseinsky, M. J. *Acc. Chem. Res.* **2005**, *38*, 273–282.
(5) Morris, R. E.; Wheatley, P. S. *Angew. Chem., Int. Ed.* **2008**, *47*, 4966–4981.
(6) Dincá, M.; Long, J. R. *Angew. Chem., Int. Ed.* **2008**, *47*, 6766–6779.
(7) Wang, Z.; Cohen, S. M. *Chem. Soc. Rev.* **2009**, *38*, 1315–1329.
(8) (a) Kondo, M.; Yoshitomi, T.; Seki, K.; Matsuzaka, H.; Kitagawa, S. *Angew. Chem., Int. Ed.* **1997**, *36*, 1725–1727. (b) Rowsell, J. L. C.; Millward, A. R.; Park, K. S.; Yaghi, O. M. *J. Am. Chem. Soc.* **2004**, *126*, 5666–5667. (c) Millward, A. R.; Yaghi, O. M. *J. Am. Chem. Soc.* **2005**, *127*, 17998–17999.
(9) (a) Mueller, U.; Schubert, M.; Teich, F.; Puetter, H.; Schierle-Arndt, K.; Pastre, J. *J. Mater. Chem.* **2006**, *16*, 626–636. (b) Li, J.; Kuppler, R. J.; Zhou, H. *Chem. Soc. Rev.* **2009**, *38*, 1477–1504. (c) Couck, S.; Denayer, J. F. M.; Baron, G. V.; Remy, T.; Gascon, J.; Kapteijn, F. *J. Am. Chem. Soc.* **2009**, *131*, 6326–6327.
(10) (a) Fujita, M.; Know, Y. J.; Washizu, S.; Ogura, K. *J. Am. Chem. Soc.* **1994**, *116*, 1151–1152. (b) Lee, J.; Farha, O. K.; Roberts, J.; Scheidt, K. A.; Nguyen, S. T.; Hupp, J. T. *Chem. Soc. Rev.* **2009**, *38*, 1450–1459. (c) Ma, L.; Abney, C.; Lin, W. *Chem. Soc. Rev.* **2009**, *38*, 1248–1256. (d) Hasegawa, S.; Horike, S.; Matsuda, R.; Furukawa, S.; Mochizuki, K.; Kinoshita, Y.; Kitagawa, S. *J. Am. Chem. Soc.* **2007**, *129*, 2607–2614. (e) Horike, S.; Dincá, M.; Tamaki, K.; Long, J. R. *J. Am. Chem. Soc.* **2008**, *130*, 5854–5855. (f) Juan-Alcañiz, J.; Ramos-Fernandez, E. V.; Lafont, U.; Gascon, J.; Kapteijn, F. *J. Catal.* **2010**, *269*, 229–241.

Published on Web 07/30/2010

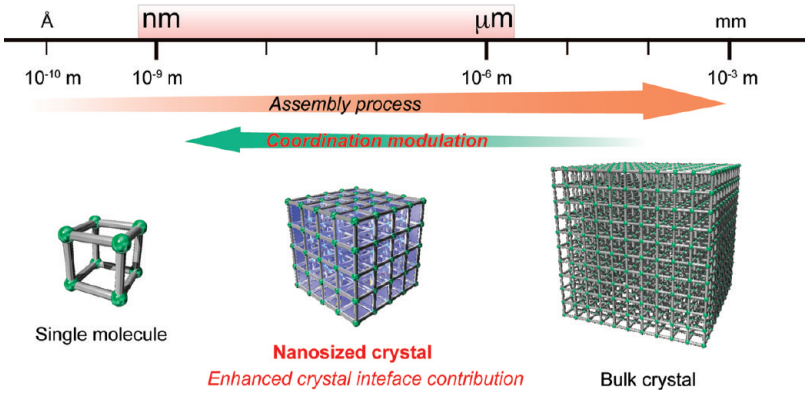

Figure 1. Schematic illustration of the importance of nanosized PCP crystals with the enhanced contribution of crystal interfaces.

sorption type. Moreover, for the nanosized porous materials, the diffusion length is decreased, which is of utmost importance in catalysis and sorption, especially in liquid phase application. Indeed, emerging fields such as porous membranes,[11] thin film devices,[12] or carrier particles for drug delivery[13] are highlighting that miniaturizing and controlling the crystal size and shape (morphology) of these porous coordination frameworks are key features to strengthen their contribution to the development of nanotechnology.[14]

In that sense, a general multiscale synthetic strategy, allowing the finely controlled formation of PCPs crystals, in the desired scale ranging from the nano regime to the lower end of the micro regime (Figure 1), may considerably facilitate their applications in various fields by providing homogeneous and tunable functional materials. Such multiscale synthesis will permit the systematic investigation of the inherent influence of the crystal surface on the porous properties. Moreover, the opportunity to take control over the rate and direction of the framework extension can provide valuable insights for a better understanding of the molecular assembly processes involved in PCPs growth mechanisms,[15,16] which is a requirement to achieve the designed synthesis of new compounds with predictable structures and properties.

Several distinct approaches have been already developed for the syntheses of crystalline nanosized PCPs, including water-in-oil microemulsions,[17] surfactant-mediated hydrothermal syntheses,[18] microwave-assisted routes,[19] and sonochemistry.[20] However, even though distinct nanocrystal sizes can be obtained by altering the experimental conditions, the precise control over a wide range of dimensions still remains challenging. We recently demonstrated a novel fabrication method for PCP nanocrystals—the so-called coordination modulation method[15]—by altering the coordination equilibrium at the crystal surface during the growth process, through competitive interactions originating from a capping additive (modulator) with the same chemical functionality as the framework linker. Although we succeeded in controlling the crystal morphology by the coordination modulation method, the fine-tuning of the crystal size still remains to be achieved.

In this study, we present a simple and straightforward strategy that combines two apparently antagonistic conditions—the coordination modulation method and microwave-assisted synthesis—to gain efficient control over the nucleation process and, thus, control over the size of the resulting PCP. We chose, as a candidate, the simplest cubic framework of $[Cu_3(btc)_2]$ (where btc represents benzene-1,3,5-tricarboxylate),[21] through the coordination modulation of a monocarboxylic acid (*n*-dodecanoic acid) additive, combined with microwave-assisted conditions. The size of crystals could be successfully tuned from 20-nm globular particles up to 2-μm cubic crystals and the correlation between the sorption properties and crystallinity of the nanoparticles confirmed that the coordination modulation method produces highly crystalline samples with high porosity, comparable to that of bulk

(11) (a) Guo, H.; Zhu, G.; Hewitt, I. J.; Qiu, S. *J. Am. Chem. Soc.* **2009**, *131*, 1646–1647. (b) Ameloot, R.; Gobechiya, E.; Uji-i, H.; Martens, J. A.; Hofkens, J.; Alaerts, L.; Sels, B. F.; De Vos, D. E. Adv. Mater. **2010**, *22*, 2685−2688.
(12) (a) Hermes, S.; Schröder, F.; Chelmowski, R.; Wöll, C.; Fischer, R. A. *J. Am. Chem. Soc.* **2005**, *127*, 13744. (b) Biemmi, E.; Scherb, C.; Bein, T. *J. Am. Chem. Soc.* **2007**, *129*, 8054–8055. (c) Gascon, J.; Aguado, S.; Kapteijn, F. *Microporous Mesoporous Mater.* **2008**, *113*, 132–138. (d) Demessence, A.; Horcajada, P.; Serre, C.; Boissiere, C.; Grosso, D.; Sanchez, C.; Ferey, G. *Chem. Commun.* **2009**, 7149–7151. (e) Allendorf, M. D.; Houk, R. J. T.; Andruszkiewicz, L.; Talin, A. A.; Pikarsky, J.; Choudhury, A.; Gall, K. A.; Hesketh, P. J. *J. Am. Chem. Soc.* **2008**, *130*, 14404–14405. (f) Zacher, D.; Shekhah, O.; Woll, C.; Fischer, R. A. *Chem. Soc. Rev.* **2009**, *38*, 1418–1429.
(13) (a) Horcajada, P.; et al. *Nat. Mater.* **2009**, *9*, 172–178. (b) Taylor-Pashow, K. M. L.; Rocca, J. D.; Xie, Z.; Tran, S.; Lin, W. *J. Am. Chem. Soc.* **2009**, *131*, 14261–14263.
(14) Lin, W.; Rieter, W.; Taylor, K. *Angew. Chem., Int. Ed.* **2009**, *48*, 650–658.
(15) Tsuruoka, T.; Furukawa, S.; Takashima, Y.; Yoshida, K.; Isoda, S.; Kitagawa, S. *Angew. Chem., Int. Ed.* **2009**, *48*, 4739–4743.
(16) (a) Spokoyny, A. M.; Kim, D.; Sumrein, A.; Mirkin, C. A. *Chem. Soc. Rev.* **2009**, *38*, 1218–1227. (b) Hermes, S.; Witte, T.; Hikov, T.; Zacher, D.; Bahnmüller, S.; Langstein, G.; Huber, K.; Fischer, R. A. *J. Am. Chem. Soc.* **2007**, *129*, 5324–5325. (c) Zacher, D.; Liu, J.; Huber, K.; Fischer, R. A. *Chem. Commun.* **2009**, 1031–1033.
(17) Rieter, W. J.; Taylor, K. M. L.; An, H.; Lin, W.; Lin, W. *J. Am. Chem. Soc.* **2006**, *128*, 9024–9025.
(18) (a) Huang, L.; Wang, H.; Chen, J.; Wang, Z.; Sun, J.; Zhao, D.; Yan, Y. *Microporous Mesoporous Mater.* **2003**, *58*, 105–114. (b) Qiu, L.; Xu, T.; Li, Z.; Wang, W.; Wu, Y.; Jiang, X.; Tian, X.; Zhang, L. *Angew. Chem., Int. Ed.* **2008**, *47*, 9487–9491.
(19) (a) Ni, Z.; Masel, R. I. *J. Am. Chem. Soc.* **2006**, *128*, 12394–12395. (b) Seo, Y.; Hundal, G.; Jang, I. T.; Hwang, Y. K.; Jun, C.; Chang, J. *Microporous Mesoporous Mater.* **2009**, *119*, 331–337.
(20) (a) Qiu, L.; Li, Z.; Wu, Y.; Wang, W.; Xu, T.; Jiang, X. *Chem. Commun.* **2008**, 3642–3644. (b) Tanaka, D.; Henke, A.; Albrecht, K.; Moeller, M.; Nakagawa, K.; Kitagawa, S.; Groll, J. *Nature Chem.* **2010**, *2*, 410–416.
(21) Chui, S. S.; Lo, S. M.; Charmant, J. P. H.; Orpen, A. G.; Williams, I. D. *Science.* **1999**, *283*, 1148–1150.

crystals obtained from optimized solvothermal methods. Interestingly, distinct gas sorption profiles, showing, for example, high affinity for surface condensation in the case of small nanoparticles with a high surface area, or even dual hierarchical porous structures presenting mesoporous grain boundaries could be observed and were correlated to the size and morphology of crystals, thus highlighting the remarkable effect of crystal size on their properties.

Experimental Section

Materials. Reagents and solvents were purchased from commercial sources and used without further purification. Microwave-assisted solvothermal reactions were performed using an Initiator 2.5 microwave from Biotage.

Preparation of $[Cu_3(btc)_2]$ Nanocrystals. In a typical experiment, copper acetate hydrate ($Cu(OAc)_2 \cdot H_2O$; 34.5 mg, 0.17 mmol) and dodecanoic acid were dissolved in butanol in a 5-mL Pyrex microwave vial. The mixture was quickly heated with a heat gun to obtain a clear solution. Benzene-1,3,5-tricarboxylic acid (20 mg, 0.095 mmol) was added at room temperature, and the sealed reaction mixture was then placed in the microwave reactor and heated to 140 °C for 10 min. The resulting blue powder was isolated by centrifugation and washed with ethanol by three dispersion−sonication−centrifugation cycles. The resulting light blue solid was dried for 1 h at 20 mmbar at room temperature before analysis.

Transmission Electron Microscopy. The TEM observations were performed with a JEOL Model JEM-1400 transmission electron microscopy (TEM) system operating at 120 kV. The TEM samples were prepared by dispersing the blue precipitates in THF, followed by depositing the solution dropwise onto a carbon-coated TEM grid. The size and size distribution of nanocrystals were measured using calibrated TEM images by ImageJ software (a public domain image processing and analysis program). For each sample, 250−500 particles were measured for the statistical size distribution analysis. The average particle size was determined by Gaussian fitting of the data.

Field-Emission Scanning Electron Microscopy. Scanning electron microscopy (SEM) observations were performed with a JEOL Model JSM-7001F4 SEM system operating at 5.0, 15.0, and 25.0 kV. Dried powder samples were deposited on carbon tape and coated with osmium prior to measurement.

Gas Sorption Measurement. The sorption isotherms of $[Cu(btc)_2]$ for nitrogen at 77 K were recorded on a BELSORP-max volumetric-adsorption instrument from BEL Japan, Inc. All measurements were performed using the samples after pretreatment at 130 °C under vacuum conditions for 12 h. Surface areas were estimated by the Brunauer−Emmett−Teller (BET) method. The mesopore size distribution was determined using the Barrett−Joyner−Halenda (BJH) method and obtained from the analysis of the adsorption branch of the isotherm.

Powder X-ray Diffraction Measurement. The diffraction data were collected on a Bruker Model D8 Discover apparatus with GADDS equipped with a sealed tube X-ray generator producing Cu Kα radiation.

Thermogravimetric Analysis. The analysis were performed using a Rigaku Model Thermo Plus TG 8120 apparatus in the temperature range of 298−773 K under a nitrogen atmosphere, at a heating rate of 5 K min^{-1}.

Results and Discussion

Our strategy to control crystal size combined microwave-assisted conditions and the coordination modulation method, which are two apparently antagonistic conditions. On the one hand, microwave-assisted heating was recently demonstrated to be an appealing route for the fast synthesis of porous coordination polymers, considerably accelerating nucleation and crystal growth processes and providing phase-pure materials with a homogeneous size distribution.[14,19] On the other hand, we expected high concentrations of monocarboxylic acid additive to efficiently slow the reaction rate of carboxylate-based PCPs through the stabilization of the monomer precursors, thus allowing the formation of highly crystalline materials. Butanol mixtures of copper acetate and benzene-1,3,5-tricarboxylate in the presence of various amounts of dodecanoic acid were reacted under microwave-assisted heating and provided phase-pure and homogeneous $[Cu_3(btc)_2]$ samples, within only 10 min, in good to high yields (60%−85%), depending on the concentration of monocarboxylic additive.

Effect of Monocarboxylic Acid Additive on Crystal Size and Morphology. In contrast to classical syntheses of HKUST-1 framework, where copper nitrate and benzene-1,3,5-tricarboxylic acid are usually reacted in water/ethanol mixtures or DMF solution,[21,22] we used butanol solvent and copper acetate as the metal source. Copper acetate is a reagent of choice because it already comprises the paddle wheel configuration of the copper dimer found in the $[Cu_3(btc)_2]$ framework.[23] Moreover, when mixed at room temperature with no additives, copper acetate and benzene-1,3,5-tricarboxylic acid readily form a blue precipitate of $[Cu_3(btc)_2]$ with low crystallinity, while with copper nitrate, high temperatures and longer reaction time are needed before the appearance of precipitate is observed. This feature suggests a faster reaction with copper acetate, which is more suitable for control through the coordination modulation.

As illustrated in Figure 2a, the addition of dodecanic acid strongly influenced the morphology of the resulting $[Cu_2(btc)_3]$ crystals and provided highly fused globular nanoparticles (~20 nm in size) when $r = 10$, where r is defined as the ratio of dodecanoic acid to benzene-1,3,5-tricarboxylic acid. Without a monocarboxylic additive, a nanocrystalline powder with ill-defined gel-like morphology was obtained.[24] The choices of monocarboxylic acid and solvent also greatly influenced the resulting morphology of the $[Cu_3(btc)_2]$ crystals. As shown in Figure 2b, in the case of the higher concentration of modulator ($r = 50$), the combination of butanol and dodecanoic acid provided nanocrystalline particles with square projections observed by TEM, reflecting their cubic morphology, as confirmed by SEM (shown in Figure 3). When

(22) Krawiec, P.; Kramer, M.; Sabo, M.; Kunschke, R.; Frode, H.; Kaskel, S. *Adv. Eng. Mater.* **2006**, *8*, 293–296.
(23) Schlesinger, M.; Schulze, S.; Hietschold, M.; Mehring, M. *Microporous Mesoporous Mater.* **2010**, *132*, 121–127.
(24) Li, Z.; Qiu, L.; Xu, T.; Wu, Y.; Wang, W.; Wu, Z.; Jiang, X. *Mater. Lett.* **2009**, *63*, 78–80.

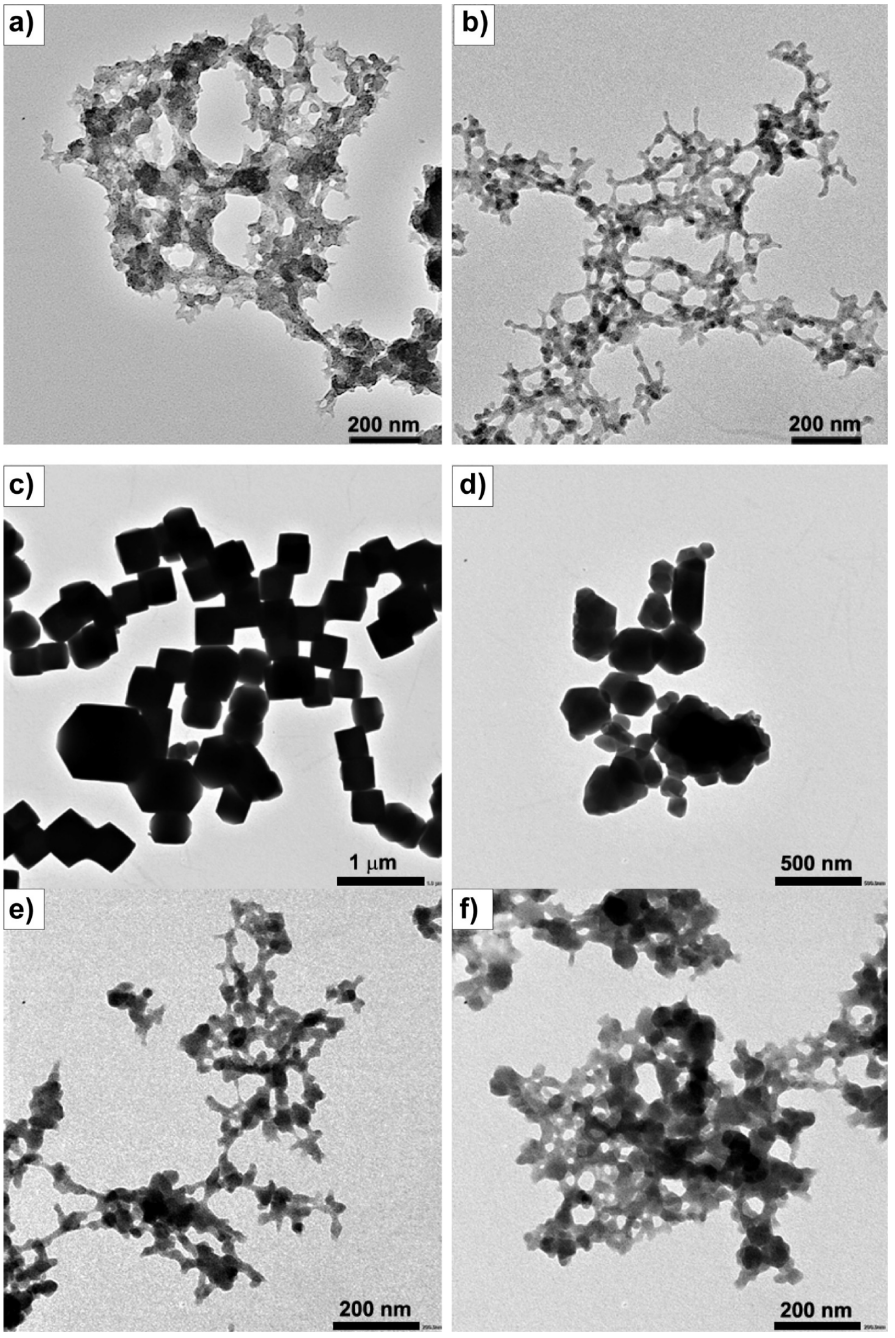

Figure 2. TEM images of $[Cu_3(btc)_2]$ samples obtained under various combination of modulator/solvent; *r* represents the ratio between monocarboxylic acid and benzene-1,3,5-tricarboxylic acid: (a) $r = 0$: butanol; (b) $r = 10$: dodecanoic acid/butanol; (c) $r = 50$: dodecanoic acid/butanol; (d) $r = 50$: acetic acid/butanol; (e) $r = 50$: dodecanoic acid/ethanol; and (f) $r = 50$: acetic acid/ethanol. All samples were prepared under microwave irradiation (140 °C, 10 min). The concentration of benzene-1,3,5-tricarboxylic acid ($c = 0.063$ M) is the same in all experiments.

dodecanoic acid was replaced by acetic acid, the resulting crystals became less defined and heterogeneous. Moreover, changing the solvent for ethanol led to highly fused particles 20−50 nm in size, regardless of the choice of modulator (either acetic acid or dodecanoic acid). From these preliminary experiments, we choose the combination of dodecanoic acid and butanol for further investigation, because they provided a slower reaction rate and bigger crystals with better defined morphology, compared to the other associations of modulator/solvent.

To gain information on the precise influence of dodecanoic acid upon the crystal growth of $[Cu_3(btc)_2]$, we carried out sets of experiments where the concentration of monocarboxylic acid was systematically varied. First, the ratio between the dodecanoic acid and benzene-1,3,5-tricarboxylic acid content was varied from $r = 25$ to $r = 75$, keeping the concentration of starting material constant (the concentration of benzene-1,3,5-tricarboxylic acid is defined as *c*). In the second set of experiments, for a given ratio ($r = 25$, 50, or 75), only the volume of solvent changed, thus affecting the global concentration. The TEM images of the resulting samples for both sets of experiments are summarized in Figure 4, and the mean sizes of the crystals are represented as a

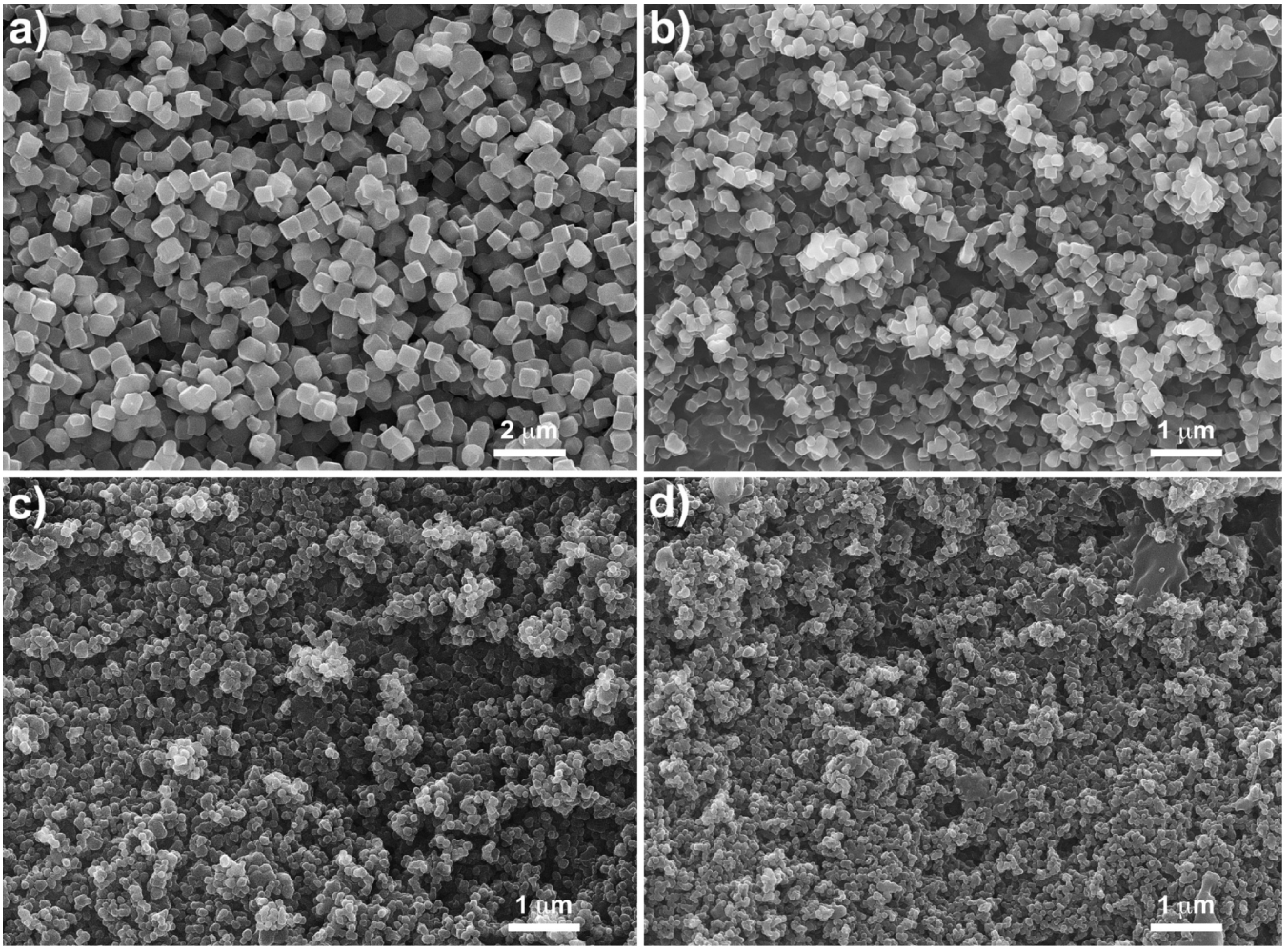

Figure 3. Field-emission scanning electron microscopy (SEM) images of $[Cu_3(btc)_2]$ samples obtained with butanol solvent, dodecanoic acid modulator, and various concentrations (c) of starting material: (a) $c = 0.063$ M; (b) $c = 0.032$ M; (c) $c = 0.016$ M; and(d) $c = 0.011$ M. The ratio between dodecanoic acid and benzene-1,3,5-tricarboxylic acid was kept constant ($r = 50$: dodecanoic acid/butanol).

function of the concentration of dodecanoic acid in Figure 5. As one could envisage, for a given ratio r, the particles became smaller when the global concentration was decreased.[19a] For example, when $r = 50$, a high concentration of starting materials ($c = 0.19$ M) afforded nanocubic crystals with an average size of 660 nm, while decreasing the initial concentration by a dilution factor of 6 ($c = 0.032$ M) lead to smaller cubic particles close to 200 nm in size. More interestingly, for a fixed concentration of starting materials, increasing the dodecanoic acid content promoted the growth of larger crystals. With an initial concentration of benzene-1,3,5-tricarboxylic acid of 0.032 M, 25 equiv of dodecanoic acid ($r = 25$) led to the formation of small fused nanoparticles ~30 nm in size. Doubling the modulator concentration ($r = 50$) while keeping the initial concentration of starting materials constant, resulted in 200 nm cubic nanocrystals, and when $r = 75$, the mean size increased close to 450 nm. Note that the largest crystals (~2 μm), were obtained with $r = 150$; however, under these conditions, the reaction was much slower and after 10 min of reaction time, almost no precipitation could be observed and a longer reaction period was required to obtained reasonable yields (see Figure S1 in the Supporting Information). This trend was verified for different concentrations of starting reagents.

Nucleation Rate Control. As summarized in Figure 5, increasing the concentration of monocarboxylic acid modulator unambiguously leads to the increased mean size of the resulting crystals. This tendency, which has already been observed with polymer additives,[25] is in opposition with conventional methods for tuning the crystal size, where higher concentrations of additives usually yield smaller crystals, because of the efficient suppression of the framework extension.[16b,26] The monocarboxylic acid is expected to efficiently influence the nucleation process by creating a competitive situation for the complexation of copper(II) cations, thus decreasing the oversaturation of the precursor materials. Although the microwave-assisted heating is known to drastically increase the rates of the nucleation and crystal growth processes, compared to classical solvothermal conditions,[19a] in the present case, high concentrations of additive can however provide a slow

(25) Uemura, T.; Hoshino, Y.; Kitagawa, S.; Yoshida, K.; Isoda, S. *Chem. Mater.* **2006**, *18*, 992–995.
(26) (a) Uemura, T.; Kitagawa, S. *J. Am. Chem. Soc.* **2003**, *125*, 7814–7815. (b) Leff, D. V.; Ohara, P. C.; Heath, J. R.; Gelbart, W. M. *J. Phys. Chem.* **1995**, *99*, 7036–7041.

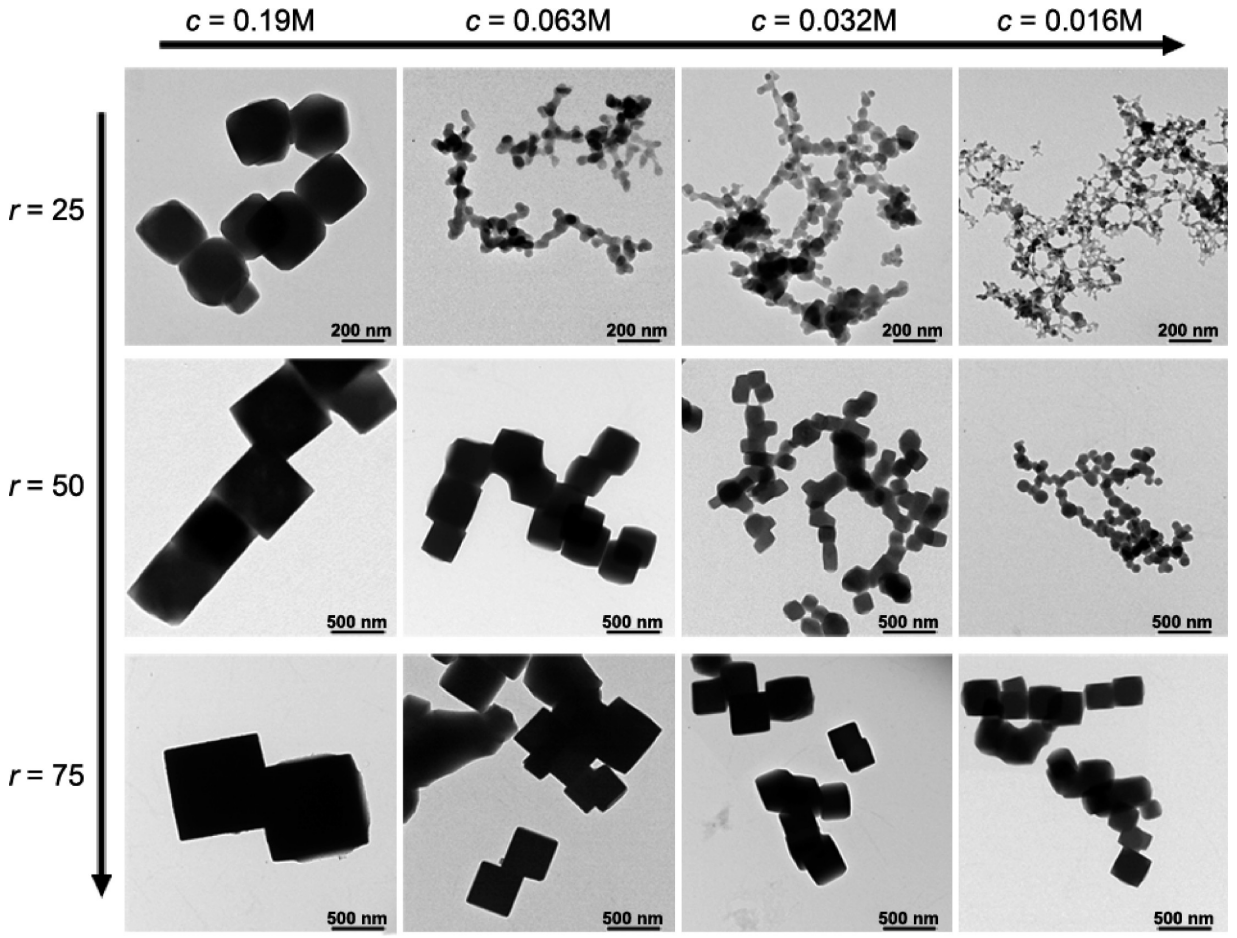

Figure 4. TEM images of samples obtained with various concentrations of dodecanoic acid and benzene-1,3,5-tricarboxylic acid. All samples were prepared under microwave irradiation (140 °C, 10 min).

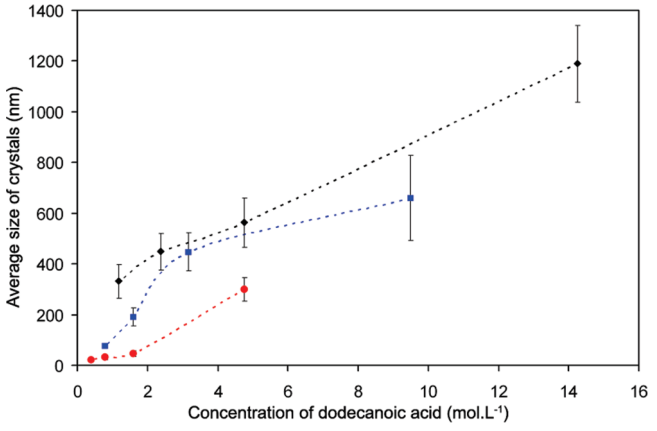

Figure 5. Average size of $[Cu_3(btc)_2]$ crystals, as a function of the concentration of dodecanoic acid: $r = 25$ (red), $r = 50$ (blue), and $r = 75$ (black).

nucleation (fewer nuclei) of the $[Cu_3(btc)_2]$ framework. A smaller number of crystals are indeed growing in line with the persistent nucleation during the heating process, leading to larger crystals with greater size polydispersity. With lower concentrations of modulator, the nucleation occurs faster. A large number of nuclei are formed and rapidly grow at the same time, while the available reagents are quickly depleted, affording smaller crystals with homogeneous size distribution (see Scheme 1).

We also monitored the evolution of reaction yield as a function of time, as shown in Figure 6. For the lower concentration of modulator ($r = 25$), high yields of products are obtained, even after very short periods (< 1 min) and this value did not evolve significantly after a prolonged heating time. On the other hand, with higher concentrations of dodecanoic acid ($r = 75$), the yield increases dramatically within the first 10 min and then more gradually. A striking feature in this case is that the crystal size does not evolve significantly after 1 min (see inset in Figure 6), while the reaction yield is more than doubled after 1 h (from 36% to 78%). This observation supports our hypothesis that dodecanic acid is efficiently affecting the formation of $[Cu_3(btc)_2]$ nuclei but does not dramatically influence the growth of crystals, which remains very fast.

Characterization and Influence of Crystal Size on Gas Sorption Properties. All samples were characterized by powder X-ray diffraction (PXRD) measurement and thermogravimetric analysis. Figure 7 shows representative PXRD patterns for the bulk sample ($r = 0$), small nanoparticles (50 nm, $r = 25$), and larger nanocrystals (1 μm, $r = 75$). In all cases, the characteristic diffractions peaks of $[Cu_3(btc)_2]$ were identified, testifying for the phase-pure formation of $[Cu_3(btc)_2]$ samples via the microwave-assisted coordination modulation method. Interestingly,

Scheme 1. Schematic Representation for the Nucleation-Controlled Formation of $[Cu_3(btc)_2]$ Nanoparticles[a]

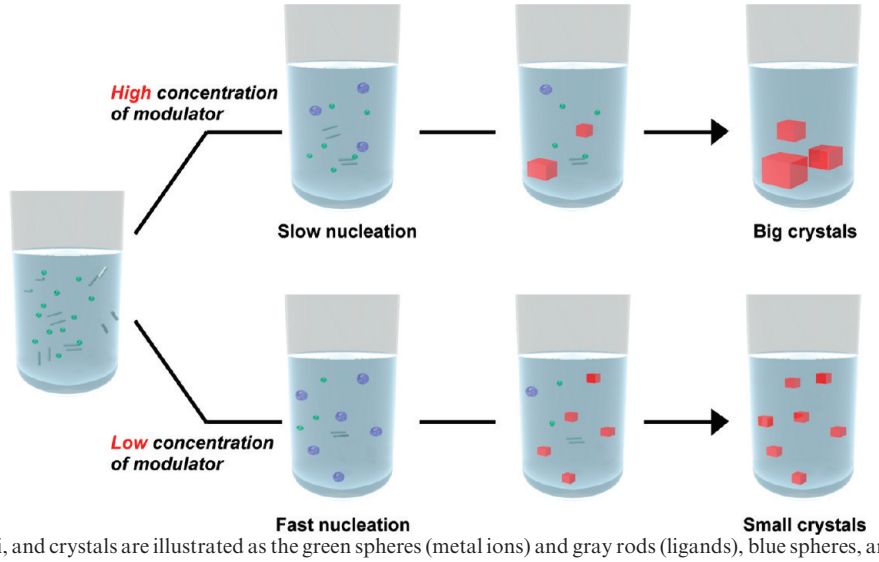

[a] The precursors, nuclei, and crystals are illustrated as the green spheres (metal ions) and gray rods (ligands), blue spheres, and red cubes, respectively.

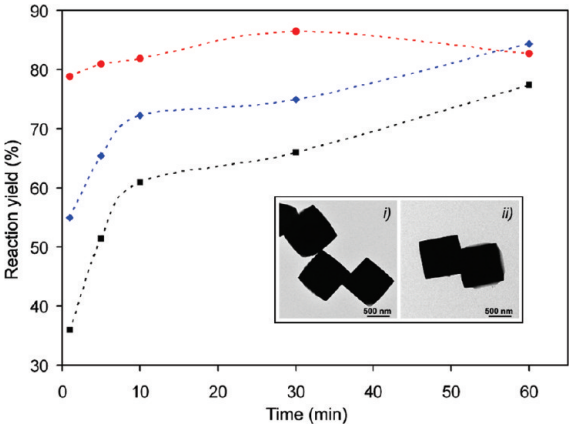

Figure 6. Reaction yield as a function of time for different concentrations of dodecanoic acid: $r = 25$ and $c = 0.063$ M (red); $r = 75$ and $c = 0.063$ M (blue); and $r = 75$ and $c = 0.19$ M (black). Inset shows TEM images of $[Cu_3(btc)_2]$ samples ($r = 75$, $c = 0.19$M) obtained after (i) 1 min and (ii) 10 min at 140 °C.

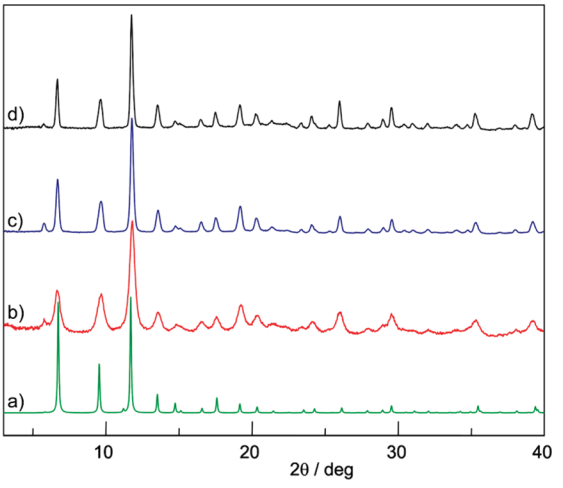

Figure 7. Powder X-ray diffraction (PXRD) patterns for representative samples: (a) simulated pattern of HKUST-1, (b) $r = 0$, (c) $r = 25$, and (d) $r = 75$. Initial concentration of benzene-1,3,5-tricarboxylic acid is 0.063 M, except for $r = 75$, where $c = 0.19$ M.

the samples synthesized in the presence of dodecanoic acid present sharp diffraction peaks, contrasting with the bulk sample ($r = 0$), where broader Bragg diffraction peaks were observed, accounting for its lower crystallinity. Despite the small size of the nanoparticles (50 nm, $r = 25$), no difference could be noticed in the diffraction peak widths when compared to those of the larger crystals (1 μm, $r = 75$), which indicates the excellent crystallinity of the nanoparticles.

The coordination modulation method with dodecanoic acid not only allows one to finely tune the size of the $[Cu_3(btc)_2]$ crystals (from 20 nm to 2 μm) through the control of the nucleation process, but it also provides materials with improved crystallinity. To demonstrate that the monocarboxylic additive could be efficiently removed from the porous framework, we checked the nitrogen adsorption properties for the same representative samples as those described above for PXRD measurement, after a simple washing process consisting of three cycles of quick sonication, centrifugation, and redispersion in ethanol. The dried samples were activated at 130 °C under vacuum for 12 h prior to sorption measurements. The adsorption isotherms of nitrogen for the samples synthesized by the coordination modulation method (Figure 8a) show the characteristic Type I sorption profiles[27] with high amount of nitrogen adsorption; both samples of the small nanoparticles (50 nm, $r = 25$) and the large crystals (1 μm, $r = 75$) present a BET surface areas of 1270 $m^2\ g^{-1}$, standing among the highest values reported for $[Cu_3(btc)_2]$.[23] Although the coordination of the monocarboxylic acid on the crystal surface is unclear, the high capacity of gas sorption suggests that the modulator is absent from the pores after the washing process and does not induce significant defects in the framework. The sorption profiles of these two crystalline

(27) Sing, K. S.; Everett, D. H.; Haul, R. A. W.; Moscou, L.; Pierotti, R. A.; Rouquerol, J.; Siemieniewska, T. *Pure Appl. Chem.* **1985**, *57*, 603–619.

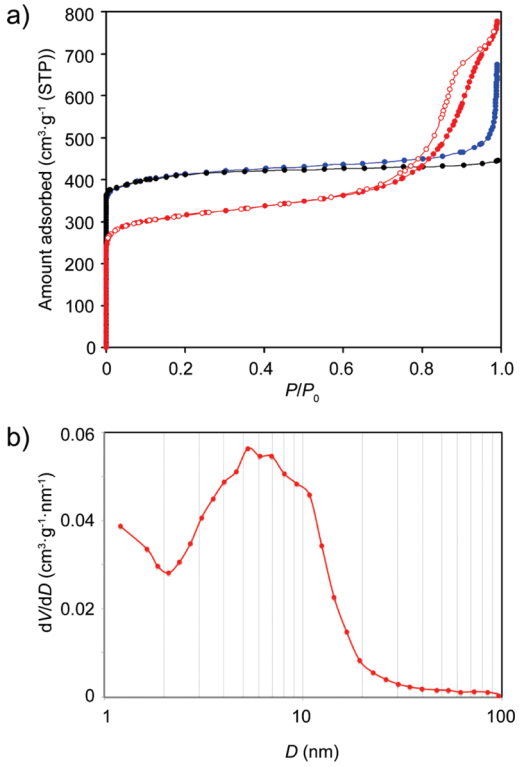

Figure 8. (a) Adsorption isotherms for nitrogen (at 77 K) of representative samples: $r = 25$ (blue); $r = 75$ (black); and $r = 0$ (red). The initial concentration of btc is 0.063 M, except for $r = 75$, where $c = 0.19$ M. For the sake of clarity, desorption profiles for $r = 25$ and 75 are not represented. (b) Pore size distribution in the mesoporous regime of the sample, showing mesoporous adsorption ($r = 0$) calculated from the adsorption isotherm.

samples are similar except in the high relative pressure region (near $P/P_0 = 1$), where the nanoparticles sample shows a sudden increase of adsorption, which can be related to physisorbed liquid nitrogen on the crystal surfaces of the nanoparticles. Such a phenomenon is not observed for the larger crystals with cubic facets, which present a much lower crystal surface area.

The bulk sample ($r = 0$) showed a very unique adsorption profile for nitrogen, i.e, the combination of the Type I microporous sorption at very low relative pressure and the Type IV mesoporous sorption with Type H2 hysteresis at the higher relative pressure.[27] The significant lower amount of nitrogen sorption (300 $cm^3\ g^{-1}$ (STP) at $P/P_0 = 0.01$), compared to the two other samples (400 $cm^3\ g^{-1}$ (STP) at $P/P_0 = 0.01$), in the lower relative pressure range is in accordance with its lower crystallinity deduced from the PXRD pattern. Interestingly, a gradual increase of the adsorbed nitrogen can be observed at higher relative pressures with a clear hysteresis for desorption, which can be recognized as the typical mesoporous sorption property. The total volume of adsorbed nitrogen (780 $cm^3\ g^{-1}$ (STP) at $P/P_0 = 1$) is much higher, compared to the available microporous volume. Such dual hierarchical porous structure in the $[Cu_3(btc)_2]$ framework was only reported for a particular case,[18b] where aggregates of surfactants were used to template the formation of mesoporous $[Cu_3(btc)_2]$. However, in the present case, no additives were used. As the crystalline state of the coordination framework shows the typical Type I microporous sorption, we conclude that the mesoporous property with the Type H2 hysteresis arises from the interstitial grain voids in the ill-defined gel-like nanoporous powder as observed by TEM measurement (see Figure 2a in this work and Figure S3 in the Supporting Information), which is also confirmed by the broad distribution of pore diameter in mesoporous regime (see Figure 8b). Thanks to the multiscale synthesis, the importance of the crystal surfaces is finally realized. The increase of the crystal surfaces area induces the condensation of nitrogen at the high relative pressure region for the small nanoparticles (50 nm, $r = 25$). More significantly, the further downsizing the PCP crystals, thus further increasing the crystal surface area ($r = 0$), allows for the physical contact between the crystal grains to form the gel-like materials that give the mesoporous property to the PCP by accumulating adsorbates in the grain voids. This hierarchical porosity has important prospects in industrial processes, such as adsorption and catalysis, because the large mesopores can enhance the diffusion of adsorbates.

Conclusion

In summary, we have presented a simple and straightforward method to efficiently control the size of $[Cu_3(btc)_2]$ crystals, ranging from few tenths of nanometers to micrometers. The microwave-assisted coordination modulation method allowed a subtle control of the nucleation rate and provided phase-pure $[Cu_3(btc)_2]$ framework with narrow size distribution. Nitrogen sorption experiments highlighted the influence of the crystal size, thus the crystal surface area, on the sorption profiles, and unusual combination of micropores and mesopores could be observed. By essence, this method is applicable to control the nucleation process of a wide range of carboxylate-based porous coordination frameworks. Furthermore, the use of functional monocarboxylic acid to decorate the surfaces of the nanocrystals is currently under investigation and will allow the fabrication of multifunctional PCP nanocrystals for more advanced applications.

Acknowledgment. We acknowledge Prof. Minoru Miyahara, Dr. Hideki Tanaka, and Dr. Daisuke Tanaka for fruitful discussions.

Supporting Information Available: Additional TEM and SEM data, particle size distribution analysis, powder X-ray diffraction, and thermogravimetric data. This material is available free of charge via the Internet at http://pubs.acs.org.